The Egyptian Journal of Radiology and Nuclear Medicine (2010) **41**, 401–409

Egyptian Society of Radiology and Nuclear Medicine

The Egyptian Journal of Radiology and Nuclear Medicine

www.elsevier.com/locate/ejrnm
www.sciencedirect.com

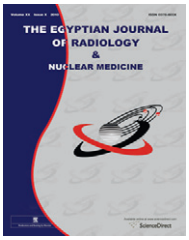

MR exponential image in ischemic stroke: A preliminary evaluation

Ghada K. Gouhar *, Tamer F. Taha

Radiodiagnosis Department, Faculty of Medicine, Zagazig University, Zagazig, Egypt

Received 8 July 2010; accepted 5 August 2010
Available online 21 October 2010

KEYWORDS

Exponential;
MR;
Stroke;
Ischemia

Abstract *Background and purpose:* Magnetic resonance (MR) diffusion images, including both the diffusion-weighted image (DWI) and the apparent diffusion coefficient (ADC), allow detection of cerebral ischemic lesions within minutes of onset, and the contrast within the image is based on microscopic motion of the water. A third type of diffusion image can be created, ''the exponential image''. Our goals were to evaluate the ability of exponential image in reflecting the changes in both DWI and ADC and whether it can replace these two sets of images in cerebral infarction patients.

Patients and methods: A total of 51 patients were enrolled in the study, 47 were included in the analysis, and four were excluded from the study. Conventional and DW MRI were performed in 47 patients. For each patient DWI, ADC maps, and exponential images were reviewed and the change in signal intensity of the lesion compared with the contralateral normal side was measured (rSI) as well as the changes in (rADC).

Results: There was a significant change in the rSI_{DW} and rSI_{Exp} in late subacute and chronic stages ($p < .001$), however, rADC showed a significant decrease ($p < .001$) in hyperacute and acute stages, followed by a significant increase ($p < .001$) in the late subacute and chronic stages. rSI_{Exp} was highly correlated with the change in the rADC values in different stages of infarction ($r = .72$, $p < .001$). However, the changes in the rSI_{DW} correlated less closely with the change in the rADC values ($r = .35$, ($p < .05$)).

* Corresponding author. Tel.: +20 0124038955.
E-mail addresses: ghadagouhar@yahoo.com, doctormona@rocketmail.com (G.K. Gouhar).

Peer review under responsibility of Egyptian Society of Radiology and Nuclear Medicine.
doi:10.1016/j.ejrnm.2010.08.001

ELSEVIER **Production and hosting by Elsevier**

Conclusion: Exponential image offers a simple, more accurate replacement for both sets (DWI and ADC), by combining the advantages of both sets.

1. Introduction

Diffusion-weighted MRI (DWI) has shown increasing potential as a probe of tissue microstructure due to its sensitivity to the restricted diffusion caused by structural barriers that limit water mobility in vivo (1,2) as first described by Stejskal and Tanner (3).

In contrast to conventional MR imaging without diffusion weighting, DW imaging provides detection of lesions in the first hours after the onset of clinical symptoms (4).

DWI allows the discrimination between lesions with increased diffusion (due to vasogenic edema) and decreased diffusion (due to cytotoxic edema). The level of diffusion weighting is indicated by the *b*-value, a parameter that reflects the length and strength of the field gradients applied in the pulse sequence (1).

Because cytotoxic edema is thought to occur early in brain ischemia, DWI is highly sensitive in the early detection of brain infarctions (5,6). It provides important pathological–physiological information as well as the possible reversibility of tissue injury (7,8). Because "time is brain," early diagnosis with early treatment is expected to improve outcome (9).

In acute cerebral ischemia, the area of restricted diffusion is identified as an area of signal increase against a hypointense background (9,10). The hyperintense appearance of acute infarcts on diffusion-weighted images results from a combination of abnormal diffusion and the intrinsic T_2 properties which is difficult to determine on diffusion-weighted images alone. Small lesion size, brainstem lesions, and small cortical lesions on DWI performed within a few hours after stroke onset were associated with a particular risk of false-negative DWI-images (11–13).

In addition, infarcts can occasionally continue to appear hyperintense on DWI in the late subacute and chronic stages (i.e., when the increase in signal intensity due to restricted water diffusion is expected to begin to decrease) because of progressive T_2 prolongation rather than a decrease in diffusion "T_2 shine-through effect" (14).

The method that measures the rate of diffusion in living systems and not the characteristics of the T_2 signal is referred to as the apparent diffusion coefficient (ADC). The ADC, a measure of the freedom of water diffusion, is believed to be low because of a shift of water, within hypoxic brain parenchyma, from the extracellular to the intracellular compartment where water diffusion is relatively restricted (15). Areas with a high diffusion will have a high ADC value and appear consequently hyperintense on the ADC maps (e.g., CSF) (9).

It is well accepted that ADC values decline rapidly after the onset of ischemia and subsequently increase and return to (pseudo)normal values, until it reaches supernormal values in a variable time course of about 17 days (16).

This technique (ADC) has drawbacks because it requires generation and interpretation of a set of ADC maps with the diffusion-weighted images. Another drawback is that these maps have different contrast characteristics from those of diffusion-weighted images to which radiologists have become accustomed (17).

To remove the T_2-weighted contrast, the DW image can be divided by the echo-planar spin-echo T_2-weighted (or $b = 0\ s/mm^2$) image to give an "exponential image" that combines the advantages of DW images and ADC maps (18).

The exponential images are a single set of MR images that show abnormal signal intensity because of restricted diffusion while negating the contribution of T_2 signal intensity to DWI, and with high lesion conspicuity (19).

The aim of this study is to evaluate the ability of MR exponential diffusion-weighted images in diagnosing cerebral infarction, and whether it can replace the combination of the two sets of diffusion-weighted images and ADC maps.

2. Patients and methods

2.1. Selection of patients

This study was conducted on 51 patients. Inclusion criteria were: patients with a presumed diagnosis of infarct age that could be accurately determined on clinical ground, and were from less than 6 h to more than 2 weeks. All patients had no contraindications to MR imaging.

Exclusion criteria were: patients with a non-ischemic lesion that could have been responsible for the symptoms, severe hemorrhage, or patients with active seizures. These criteria yielded 47 patients out of the 51 patients enrolled in the study (31 males and 16 females), the mean age range was 68 ± 11 years. A consent was taken from all patients. Four patients were excluded from the study, one patient had severe hemorrhagic infarction which interfered with image interpretation, two patients were uncertain about the time of the symptom onset, and one patient refused to complete the examination.

2.2. MRI

MRI was performed on a 1.5-T unit with (Philips Achieva System) with echo-planar capability. We performed the *standard MRI examination* as follows: axial T_1 (TR148-97/TE2-15), axial T_2 (TR4400-4800/TE110), axial flair (TR6000/TE120-TI2000).The imaging parameters were: matrix size was 256×128. Section thickness was 5 mm with a gap of 1 mm. The number of sections was set to include the whole brain (average, 22). *DWI* examination was acquired using a multisection, single-shot echo-planar imaging sequence, we used the same section thickness, interslice gap and number of sections as a standard MRI examination, with parameters of (TR 3100-3400/TE 98-99). For each slice, two diffusion weightings ($b = 0$ and $b = 1000\ mm^2/s$) were applied along the *x*, *y*, and *z* axes, scanning time was 1 min 15 s. *ADC* maps (apparent diffusion coefficient) were automatically calculated by MRI machine software and included in the sequence of DW imaging. *Exponential images* were obtained

Table 1 Shows relative signal intensity in DWI (rSI_{DWI}), relative signal intensity in exponential images (rSI_{Exp}), and relative ADC (rADC) in different stages of infarction.

Stage of infarction	No. of patients	rSI_{DWI} $b = 1000$ (mean ± SD)	$rSI_{Exponential\ image}$ (mean ± SD)	rADCm (mean ± SD)
Hyperacute stage	13	1.87 ± 0.21	1.46 ± 0.22	0.602 ± 0.07
Acute stage	11	1.96 ± 0.26	1.57 ± 0.24	0.451 ± 0.05
Early subacute stage	8	1.76 ± 0.18	1.33 ± 0.12	0.723 ± 0.09
Late subacute stage	6	1.43 ± 0.21	1.14 ± 0.13	1.061 ± 0.03
Chronic stage	9	0.96 ± 0.18	0.62 ± 0.27	2.198 ± 0.07

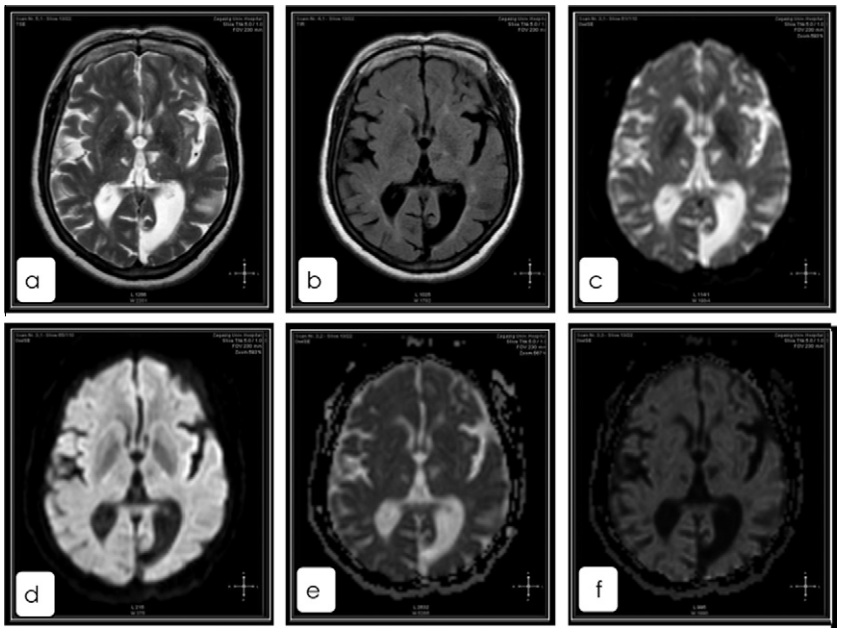

Fig. 1 Chronic infarction after 3 months of symptoms. There are two small well-defined infarctions at both thalami displaying high signal intensity at T2WI (a), DWI-b = 0 (c) and low SI at FLAIR (b). The lesions display intermediate SI at DWI-b = 1000 (d) and high SI at ADC map (e). At exponential image (f) they display low signal intensity denoting chronic infarction.

automatically by dividing the DWI by the echo-planar spin-echo T_2-weighted (or $b = 50\ s/mm^2$) image to remove the T_2-weighted contrast.

The regions of ischemic lesion on the DWI ($b = 1000$), the exponential images, and on the ADC maps were analyzed by manually outlining the regions of interest (ROI) on the lesion and the corresponding normal contralateral tissue; then the relative SIs (rSI_{DWI} and rSI_{Exp}) and the relative ADCs (rADC) quotients of the lesion and control values were calculated.

2.3. Statistical analysis

Statistical analysis was done using SPSS version 13. The mean and standard deviation were calculated for the rSIs and rADCs of each lesion. One-way analysis of variance (ANOVA test) for comparison between several means and LSD for least significance difference were done. The probability (p value) was considered non-significant when $p > .05$, significant when ($p < 0.5$), and highly significant when $p < .001$. Finally, we correlated the mean change in signal intensity on both diffusion-weighted images and exponential images with the change in the ADC using Spearman rank correlations.

3. Results

Fifty-one patients were enrolled in the study, and 47 were included in the analysis (31 males and 16 females), the mean age range was 68 ± 11 years. Four patients did not meet the criteria of patient selection and were excluded from the study, one patient had severe hemorrhagic infarction which interfered with image interpretation, two patients were uncertain about the time of the symptom onset, and one patient refuse to complete the examination. Based on clinical background and duration of symptom onset, thirteen patients had hyperacute infarcts (less than 6 h duration), eleven patients had acute infarcts (6–24 h), eight patients had early subacute infarcts (1–7 days), six patients had late subacute infarcts (less than 2 weeks duration), and nine patients had chronic infarcts (more than 2 weeks duration-up to 37 days).

In all patients, the changes in SI_{DWI} of the infarct (compared with those of normal tissue) were significantly higher ($p < 0.001$) than in SI_{Exp} images.

The rSI_{DWI} (Table 1) showed a progressive increase from hyperacute infarcts (1.87 ± 0.21) (Fig. 3) to acute infarcts (1.96 ± 0.26) (Figs. 5, 6). In the early subacute stage, the rSI_{DWI} showed no significant decrease ($p > 0.05$) (1.76 ±

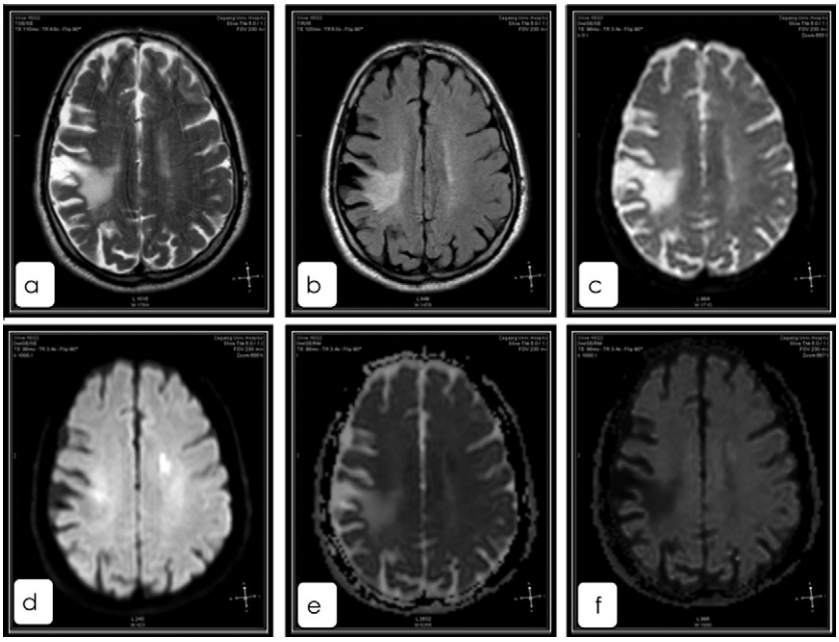

Fig. 2 Chronic infarction 6 months after symptoms. Axial T2WI (a), FLAIR (b) and DWI-b = 0 (c) show hyperintense area of infarction at the right posterior parietal region, and of intermediate signal intensity at DWI-b = 1000 (d) and high signal intensity at ADC map (e). At exponential image (f) the lesion displays low signal intensity denoting chronic infarction.

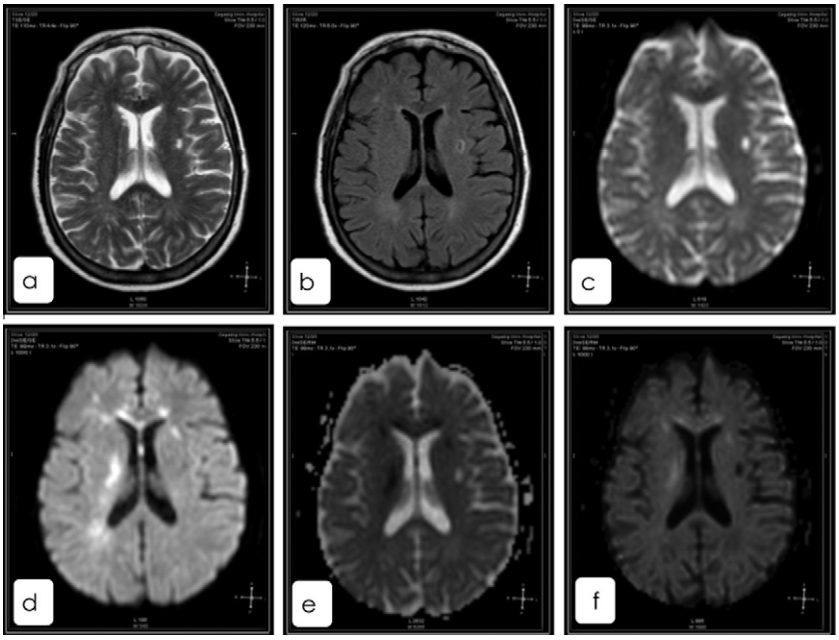

Fig. 3 Multiple hyperacute right periventricular infarctions after 5 h of symptoms. The lesions cannot be detected at axial T2WI (a), FLAIR (b) and DWI-b = 0 (c) however at DWI-b = 1000 (d) they display marked hyperintensity, and low signal intensity at ADC map (e). The lesions display high signal intensity at exponential image (f) denoting hyperacute infarction. Another associated left periventricular chronic lacunar infarct which is of high SI at T2WI, FLAIR, DWI-b = 0 and ADC map, intermediate signal intensity at DWI-b = 1000 and low SI at exponential image denoting chronic infarction.

0.18); however in late subacute (Fig. 8) and chronic (Figs. 1, 2, 4) stages a significant progressive reduction ($p < 0.001$) was seen in the rSI_{DWI} (1.43 ± 0.21 and 0.96 ± 0.18, respectively).

The mean rSI_{Exp} (Table 1) showed a progressive increase from hyperacute infarcts (1.46 ± 0.22) to acute infarcts (markedly hyperintense, 1.57 ± 0.24), with no significant

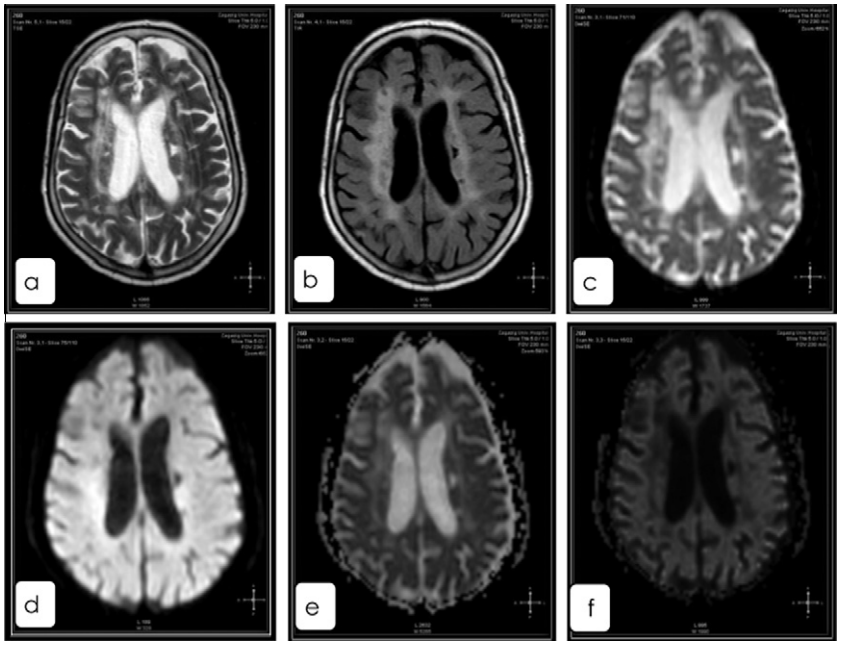

Fig. 4 T_2 "shine through" in subcortical arteriosclerotic encephalopathy patient show multiple small infarcts of high signal intensity seen at the periventicular regions displaying high SI at T2WI (a), FLAIR (b), DWI-b = 0 (c), DWI-b = 1000 (d) and ADC map (e) however it is of low SI at exponential image (f) denoting chronic infarcts. These findings are consistent with elevated diffusion secondary to microangiopathic change rather than acute infarction suggested by the DWI-images alone. Another solitary chronic left periventricular lacunar infarction of high SI at T2WI, DWI-b = 0 and ADC map and of low SI at FLAIR, DWI-b = 1000 and exponential images denoting chronic infarction.

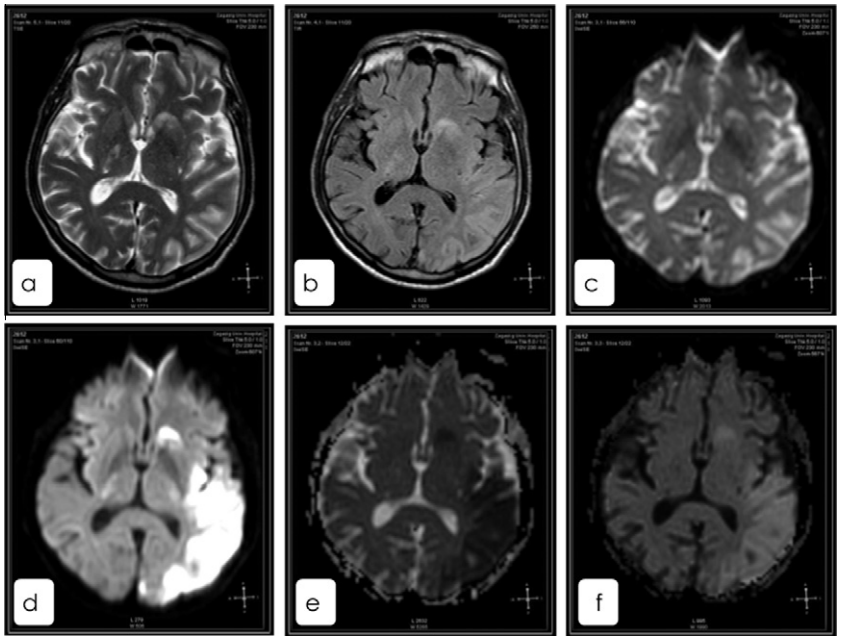

Fig. 5 Acute infarction after 8 h of symptoms at the left cortical parieto-occipital region. Axial T2WI (a), FLAIR (b) and DWI-b = 0 (c) show subtle increase in SI at the site of infarction. The lesion displays marked hyperintensity at DWI-b = 1000 (d) and low signal intensity at ADC map (e). At exponential image (f) it is of high signal intensity denoting acute infarction.

decrease ($p > 0.05$) (1.33 ± 0.12) in the early subacute infarcts. Both the late subacute (iso-intense) and chronic stages (hypointense) showed a significant progressive ($p < 0.001$) reduction in the mean rSI_{Exp} (1.14 ± 0.13 and 0.62 ± 0.27, respectively).

The mean rADC (Table 1) showed a progressive significant decrease ($p < 0.001$) in hyperacute and acute stages (0.602 ± 0.07and 0.451 ± 0.05, respectively), this was followed by gradual increase from 0.723 ± 0.09 in the early subacute stage to a

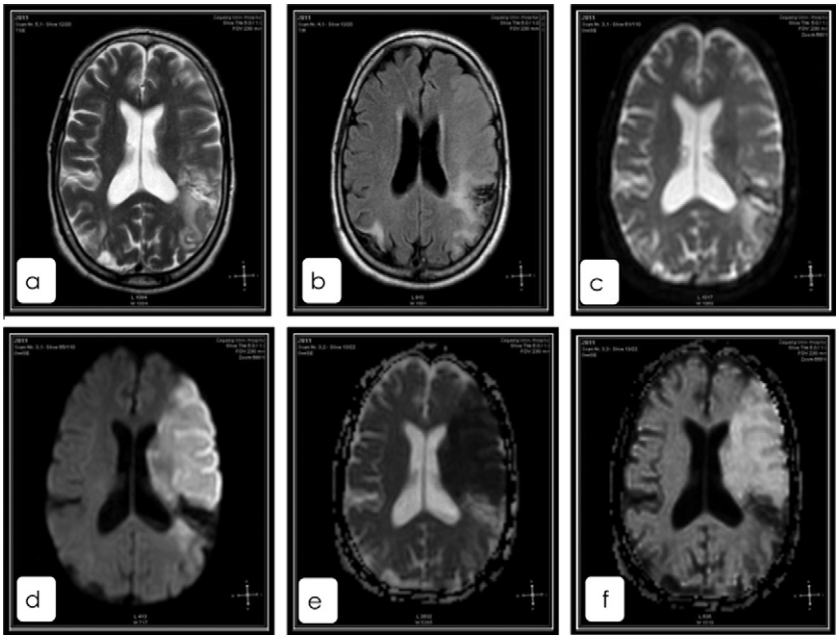

Fig. 6 Acute infarction after 7 h of symptoms at the left parietal region. Axial T2WI (a), FLAIR (b) and DWI-b = 0 (c) show subtle increase in SI at the left parietal region. The infarction is of marked hyperintensity at DWI-b = 1000 (d) and it is of low signal intensity at ADC map (e). At exponential image it is of high signal intensity denoting acute infarction. Another chronic infarction posterior to the acute one which is of high SI at T2WI, FLAIR, DWI-b = 0 and ADC and of low SI at DWI-b = 1000 and exponential image denoting chronic infarction.

Table 2 Shows Spearman rank correlation coefficient of rSI_{DWI} and rADC, and rSI_{Exp} and rADC in 47 patients.

rSI	rADC	
	Correlation coefficient (r)	Probability value (p)
rSI_{DWI}	0.35	>0.05
rSI_{Exp}	0.72	>0.001

significant increase ($p < 0.001$) reaching a pseudonormal level in the late subacute (1.061 ± 0.03), and a supernormal level in chronic stages (2.198 ± 0.07) The change in the rSI_{Exp} was highly correlated with the change in the rADC values in different stages of infarction ($r = 0.72$, $p < .001$) (Table 2). However, the changes in the rSI_{DW} correlated less closely with the change in the rADC values ($r = 0.35$, $p < .05$) (Table 2).

4. Discussion

The diagnosis of acute ischemic stroke by the use of conventional MR sequences is limited because of their relative insensitivity during the initial onset of neurologic deficit (20,21). Diffusion-weighted MR imaging has been shown to be an early marker for developing infarction (22–24) and rapidly becoming an integral part of the diagnostic workup in the acute stroke setting, as it is possible to identify severely ischemic brain regions within minutes to hours after stroke onset with a relatively high sensitivity and specifity (25–27).

In human brain the ADC decreased rapidly as early as 30 min after vascular occlusion, and continues to decrease with peak signal reduction at 1–4 days (hyperacute and acute stages). The reduction in ADC is mainly due to cytotoxic edema associated with decreased diffusion, so the lesion appears hypointense on ADC, hyperintense on DWI and less hyperintense on exponential images. The ADC returns to pseudonormal values after 1–2 weeks. This stage (subacute) is consistent with both cytotoxic edema (restricted diffusion) and vasogenic edema (increased diffusion); at this stage the lesion is mildly hyperintense on DWI due to water diffusibility and T_2 component (T_2 shine through) and iso-intense on ADC and exponential images. Subsequently, supranormal values of ADC are seen at chronic stage (more than 2 weeks), and it is attributed to increased extracellular water, tissue cavitation and gliosis, the lesion appears iso- to slight hypointense on DWI, hyperintense on ADC maps and hypointense on exponential images (28–30).

Our study (Table 1) agreed with the previous studies (14,28–32) regarding the evolution of ADC, DWI, and exponential signal intensity in different stages of infarction.

The exponential images have the advantage of showing the abnormal signal intensity because of restricted diffusion while negating the contribution of T2 signal intensity to diffusion-weighted images. These images retain the hyperintense signal characteristics of infarcts as seen on diffusion-weighted images to which radiologists have grown accustomed. Whereas on an ADC map, an acute infarct is seen as a hypointense region against an intermediate signal intensity background with relatively poor lesion conspicuity; on exponential images, an acute infarct is seen as a hyperintense lesion against a background of intermediate signal intensity normal brain tissue with high lesion conspicuity (17).

In one study (32) application of an IR pulse to suppress the CSF signal resulted in lower ADC values. This strongly suggests that the ADC values obtained from a conventional

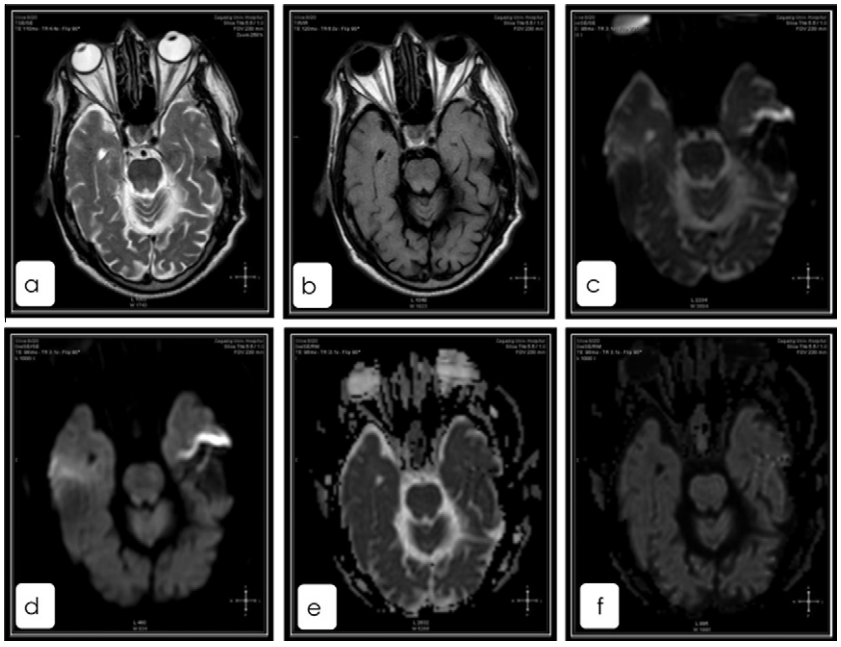

Fig. 7 T_2 "shine through". No abnormality could be detected at T2WI (a), FLAIR (b) images and ADC map (e). However, DWI-b = 0 (c) and DWI-b = 1000 (d) show hyperintense area in the left temporal region. At exponential image (f) the hyperintense left temporal area is no longer seen denoting T_2 shine-through effect seen by DWI and eliminated by exponential image.

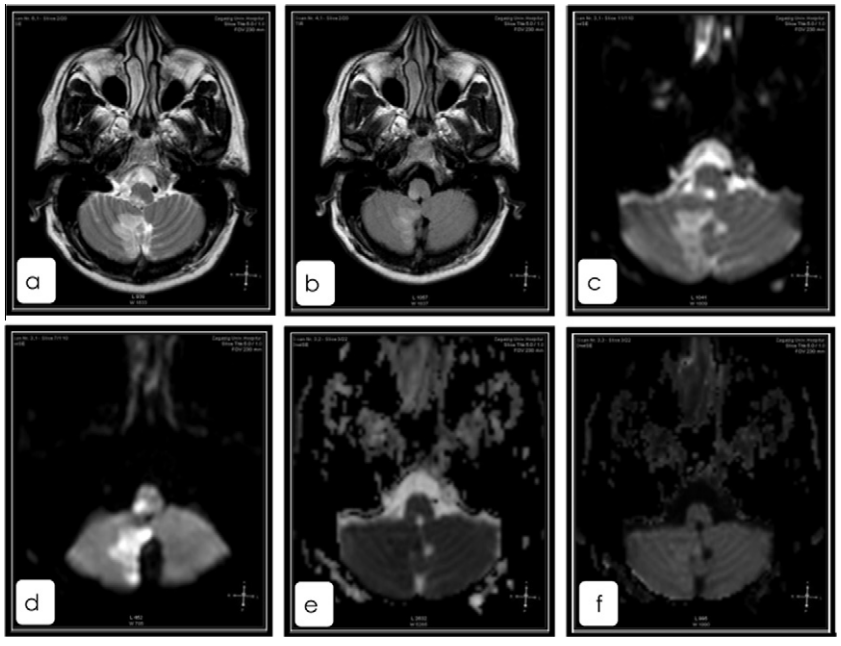

Fig. 8 Late subacute infarction after 8 days of symptoms. Axial T2WI (b), FLAIR (c) and DWI-b = 0 (c) show two hyperintense areas of infarctions at the medial aspect of the right cerebellar hemisphere and right lateral aspect of the medulla oblongata. The lesions display high SI at DWI-b = 1000 (d) and intermediate SI at ADC map (e). At exponential image (f) it displays iso-intense signal denoting late subacute infarctions.

ADC map are contaminated with CSF signal, an issue first addressed by Pierpaoli et al. (33). Thus, the IR pulse may be required to obtain accurate ADC values. Moreover, chronic lesions are frequently better visualized on the FLAIR ADC map than on the conventional ADC map (32).

On exponential images the removal of the T_2 signal intensity contribution (Fig. 7) moderately lowered signal intensity

of infarcts compared with that on diffusion-weighted images, however, the lesion conspicuity was sufficient in all cases to allow identification of infarcts.

This agreed with our study, where the lesion conspicuity on exponential images alone (without DWI or ADC) was sufficient in all cases as we could detect and determine the different types of infarction in the examined patients.

Because only a single set of images is needed, exponential images are easier to use than a combination of trace diffusion-weighted images and ADC maps (17). In addition, because the contrast characteristics of exponential images are similar to those of diffusion-weighted images, the imaging findings are similar to those to which radiologists have grown accustomed. Finally, exponential images can be used to more precisely determine the presence of restricted water diffusion, which should help to increase the accuracy of estimating the age of cerebral infarcts (17). Exponential image offers a simple solution to the common pitfalls in DWI or ADC map (34).

In conclusion exponential image can detect area with restricted diffusion more accurately as it combines the advantages of both DWI and ADC,by removing the" T_2 shine-through effect" in DWI, and higher lesion conspicuity without CSF contamination seen on ADC. Image interpretation is much more easier if we use Exponential image, as one can revise a single set of images instead of two sets (DWI and ADC) with more familiar images (similar to DWI) and higher contrast (than on ADC). One can state at the moment that exponential image offers promising and reliable images that can replace both DWI and ADC in diagnosing patients with infarction.

References

(1) Peled Sharon, Whalen Stephen, Jolesz Frence A, Golby Alexandra J. High b-value apparent diffusion-weighted images from CURVE ball DTI. J Magn Reson Imaging 2009;30(1):243–8.

(2) Rajeshkannan R, Moorthy S, Sreekumar KP, Rupa R, Prabhu NK. Clinical application of diffusion weighted MR imaging: a review. Ind J Radiol Imag 2006;16(4):705–10.

(3) Stejskal EO, Tanner JE. Spin diffusion measurements: spin echo in the presence of a time dependent field gradient. J Chem Phys 1965;42:288–92.

(4) Wessels T, Wessel C, Ellsiepen A, Reuter I, Trittmacher S, Stolz E, et al. Contribution of diffusion-weighted imaging in determination of stroke etiology. AJNR 2006;27:35–9.

(5) Desmond PM, Lovell AC, Rawlinson AA, Yang Q. The value of apparent diffusion coefficient maps in early cerebral ischemia. AJNR 2001;22:1260–7.

(6) Gonzalez RG, Schaefer PW, Buonanno FS, Schwamm LH, Budzik RF, Rordorf G, Wang B, Sorensen AG, Koroshetz WJ. Diffusion-weighted MR imaging: diagnostic accuracy in patients imaged within 6 hours of stroke symptom onset. Radiology 1999;210:155–62.

(7) Lansberg MG, Thijs VN, O'Brien MW, Ali JO, Cresping AJ, Tong DC, Moseley ME, Albert GW. Evolution of apparat diffusion coefficient, diffusion-weighted and T_2 weighted signal intensity of acute stroke. AJNR 2001;22:637–44.

(8) Karanon JO, Liu Y, Vanninen RL, Ostergaard L, Nuutien J, Roivainen R, Soimakallio PLK, Kuikka JT, Aronen HJ. Combined perfusion and diffusion weighted MR imaging in acute ischemic stroke during the 1st week. Radiology 2000;217:886–94.

(9) Huisman Thierry AGM. Diffusion-weighted imaging basic concepts and application in cerebral stroke and head trauma. Eur Radiol 2003;13:2283–97.

(10) Surikova Irina, Meisel Stefanie, Siebler Mario, Wittsack Hans-Jorg, Seitz Rudiger J. Significance of the perfusion diffusion mismatch in chronic cerebral ischemia. J Magn Reson Imaging 2006;24:771–8.

(11) Oppenheim C, Stanescu R, Dormont D, et al. False-negative diffusion-weighted MR indings in acute ischemic stroke. AJNR Am J Neuroradiol 2000;21(8):1434–40.

(12) Engelter ST, Wetzel SG, Radue EW, Rausch M, Steck AJ, Lyrer PA. The clinical significance of diffusion-weighted MR imaging in infratentorial strokes. Neurology 2004;62(4):574–80.

(13) Kueker W, Weise J, Krapf H, Schmidt F, Friese S, Baehr M. MRI characteristics of acute and subacute brainstem and thalamic infarctions: value of T2- and diffusion-weighted sequences. J Neurol 2002;249:33–42.

(14) Gonzalez RG, Hirsch JA, Koroshetz WJ, Lev MH, Schaefer P. Diffusion weighted MR imaging: diagnostic accuracy in patients imaged within 6 hours of stroke symptom onset. Radiology 2006;210:155–62.

(15) Chen PE, Simon JE, Hill MD, Sohn CH, Dickhoff P, Morrish WF, Sevick RJ, Frayne R. Acute ischemic stroke: accuracy of diffusion weighted MR imaging-effects of b-value and cerebrospinal fluid suppression. Radiology 2006;238(1): 232–9.

(16) Seitz Rudiger J, Meisel Stefanie, Weller Patrick, Junghans Ulrich, Wittsack Hans-Jorg, Siebler Mario. Initial ischemic event: perfusion-weighted MR imaging and apparent diffusion coefficient for stroke evolution. Radiology 2005;237:1020–8.

(17) Provenzale James M, Engelter Stefan I, Petrella Jeffrey R, Smith Jean S, MacFall James A. Use of MR exponential diffusion-weighted images to eradicate T2 "shine-through" effect. AJR 1999;172:537–9.

(18) Schaefer Pamela W, Ellen Grant P, Gilberto Gonzalez R. Diffusion-weighted MR imaging of the brain. Radiology 2000;217:331–45.

(19) Engelter Stefan T, Wetzel Stephan G, Bonati Leo H, Fluri Felix, Lyrer Philippe A. The clinical significance of diffusion-weighted MR imaging in stroke and TIA patients. Swiss Med Wkly 2008;138:729–40.

(20) Srinivasan A, Goyal M, Al Azri F, Lum C. State of art: imaging of acute stroke. Radiographics 2006;26:75–96.

(21) Mullins ME. Modern emergent stroke imaging: pearls, protocol, and pitfalls. Radiol Clin North Am 2006;44:41–62.

(22) Wessels T, Wessels C, Ellsiepen A, Reuter I, Trittmacher S, Stolz E, Jauss M. Contribution of diffusion-weighted imaging in determination of stroke etiology. AJNR 2005;27:35–9.

(23) Sunshine Jeffrey L, Bambakidis Nicholas, Tarr Robert W, Lanzieri Charles F, Zaidat Osama O, Suarez Jose I, et al. Benefits of perfusion MR imaging relative to diffusion mr imaging in the diagnosis and treatment of hyperacute stroke. AJNR 2001;22:915–21.

(24) Winbeck Kerstin, Bruckmaier Kathrin, Etgen Thorleif, von Einsiedel Helga Grafin, Rottinger M, Sander Dirk. Transient ischemic attack and stroke can be differentiated by analyzing early diffusion-weighted imaging signal intensity changes. Stroke 2004;35:1095–9.

(25) Ostergaard L. Principles of cerebral perfusion imaging by bolus tracking. J Mag Reson Imaging 2005;22:710–7.

(26) Wittsack HJ, Ritzl A, Fink GR, et al. MR imaging in acute stroke diffusion-weighted and perfusion imaging parameters for predicting infarct size. Radiology 2002;222:397–403.

(27) Neumann-Haefelin Tobias, Wittsack Hans-Jorg, Wenserski Frank, Siebler Mario, Seitz Rudiger J, Modder Ulrich, et al. Diffusion- and perfusion-weighted MRI. The DWI/PWI mismatch region in acute stroke. Stroke 1999;30:1591–7.

(28) Moon WJ, Wa DG, Ryoo JW, Roh HG. Assessment of tissue viability using diffusion and perfusion weighted MRI in hyperacute stroke. Korean J Radiol 2005;6(2):75–81.

(29) Kim HJ, Choi CG, Lee DH, Lee JH, Kim SJ, Suh DC. High b-value diffusion MR imaging of hyperacute ischemic stroke at 1.5 T. AJNR 2005;26:208–15.
(30) Mullins ME, Schaefer PW, Sorensen AG, Halpern EF, Ay H, He J, et al. CT and conventional and diffusion-weighted MR imaging in acute stroke: study in 691 at presentation to the emergency department. Radiology 2002;224:353–60.
(31) Somford DM, Marks MP, Thijs VN, Tong DC. Association with early CT abnormalities, infarct size and apparent diffusion coefficient reduction in acute ischemic stroke. AJNR 2004;25:933–8.
(32) Lansberg Maarten G, Thijs Vincent N, O'Brien Michael W, Ali Juan O, de Crespigny Alex J, Tong David C, et al. Evolution of apparent diffusion coefficient diffusion-weighted, and T2-weighted signal intensity of acute stroke. AJNR 2001;22:637–44.
(33) Pierpaoli C, Alger JR, Righini A, et al. High temporal resolution diffusion MRI of global cerebral ischemia and reperfusion. J Cereb Blood Flow Metab 1996;16:892–905.
(34) Dow-M K, David JC. Diffusion-weighted MRI in the body: applications and challenges in oncology. AJR 2007;188: 1622–35.